

is 90° and a second 60° according to the construction of Fig. 1, so the third angle is 30°. This results in the proportion

$$(p_A - p_{A1})/(p_{A2} - p_{A1}) = (p_B - p_{B1})/(p_{B2} - p_{B1}) \quad (\text{Eq. 2})$$

Multiplying out and simplifying result in

$$p_A p_{B2} - p_{A1} p_{B2} - p_A p_{B1} - p_{A2} p_B + p_{A1} p_B + p_{A2} p_{B1} = 0 \quad (\text{Eq. 3})$$

This is identical with

$$\begin{vmatrix} p_A & p_B & 1 \\ p_{A1} & p_{B1} & 1 \\ p_{A2} & p_{B2} & 1 \end{vmatrix} = 0 \quad (\text{Eq. 4})$$

This last expression is equivalent to those of another method of extrapolation (7), as it should be since both are solutions of the same problem. The present method has the advantage of being more direct. By applying Eq. 4 to two or more systems having convergent tie lines, the composition of the pure solid phase is obtained. If the data for several tie lines are available, the best fit for the composition corresponding to their common intersection can be calculated by least-squares analysis (8, 9). This minimizes the effect of random analytical errors.

- (1) A. H. Goldberg, M. Gibaldi, and J. L. Kanig, *J. Pharm. Sci.*, **54**, 1145(1965).
- (2) N. K. Patel, *Amer. J. Pharm. Educ.*, **34**, 47(1970).
- (3) A. N. Martin, J. Swarbrick, and A. Cammarata, "Physical Pharmacy," Lea & Febiger, Philadelphia, Pa., 1969, pp. 93-99.
- (4) J. E. Ricci, "The Phase Rule and Heterogeneous Equilibrium," D. Van Nostrand, Princeton, N. J., 1951, p. 323.
- (5) A. E. Hill and J. E. Ricci, *J. Amer. Chem. Soc.*, **53**, 4305 (1931).
- (6) F. F. Purdon and V. W. Slater, "Aqueous Solution and the Phase Diagram," Edward Arnold & Co., London, England, 1946, p. 65.
- (7) H. Schott, *J. Chem. Eng. Data*, **6**, 324(1961).
- (8) R. L. Anderson and T. A. Bancroft, "Statistical Theory in Research," McGraw-Hill, New York, N. Y., 1952, chaps. 14 and 15.
- (9) O. L. Davies, "Statistical Methods in Research and Production," 3rd ed., Hafner, New York, N. Y., 1961, Appendix 8B.

HANS SCHOTT
School of Pharmacy
Temple University
Philadelphia, PA 19140

Received May 22, 1970.

Accepted for publication September 15, 1970.

Compaction Effect on Flow Property Indexes for Powders

Keyphrases Flow property indexes—compaction effect Compaction effect—flow indexes accuracy

Sir:

Powder technologists are reluctant to suggest a single figure to describe the flow properties of a powder since it is recognized that many factors such as moisture,

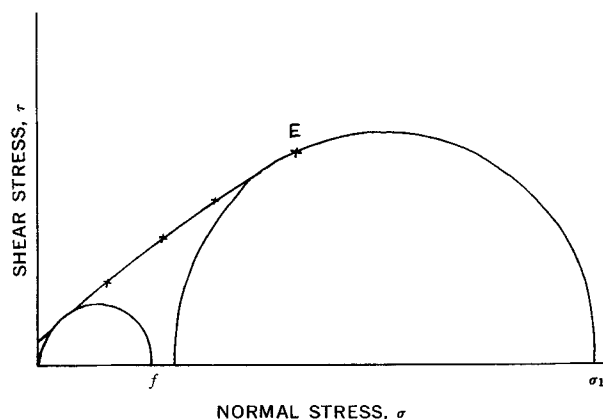


Figure 1—Idealized Jenike yield locus.

temperature, degradation, and time affect flow properties. Manufacturers, on the other hand, require a simple measure of the flow properties of their powders for process control—hence, the prevalent use of the much criticized angle of repose tests.

Two methods, both based on results obtained from a shear cell, have been suggested for characterizing powders with regard to their flow properties. The method of Jenike *et al.* (1) is called the flow factor, while that of Ashton *et al.* (2, 3) is termed the shear index.

Consider a yield locus, as shown in Fig. 1, which is obtained in the normal manner using a shear cell (1). Two Mohr circles are drawn, one passing through the origin and tangential to the locus and the other tangential to and passing through the end-point of the locus.

The basis of the Jenike flow factor, ff , is that the unconfined yield strength, f , of a powder is a function of the consolidating stress, σ_1 , applied during the sample preparation. Small values of f in relation to the value of σ_1 will indicate a free-flowing material. The flow factor, ff , is taken as the ratio σ_1/f . It is found that values of ff generally range between 1 for highly cohesive powders and 10 for free-flowing powder.

If a family of yield loci are produced at a series of compaction levels and the values of f and σ_1 are measured for each locus, it is found that the flow factor usually increases with increasing compaction.

When the shear cell is used in conjunction with a tensile tester, the end-point of the locus on the negative portion of the normal stress axis (the tensile strength T) may be plotted. Thus the complete locus can be drawn as shown in Fig. 2. It was shown by Ashton *et al.* (2)

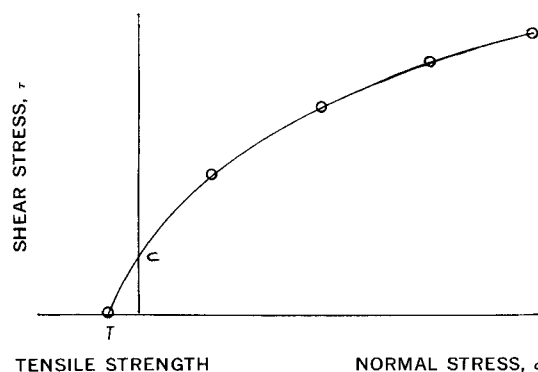


Figure 2—Complete yield locus including tensile strength.

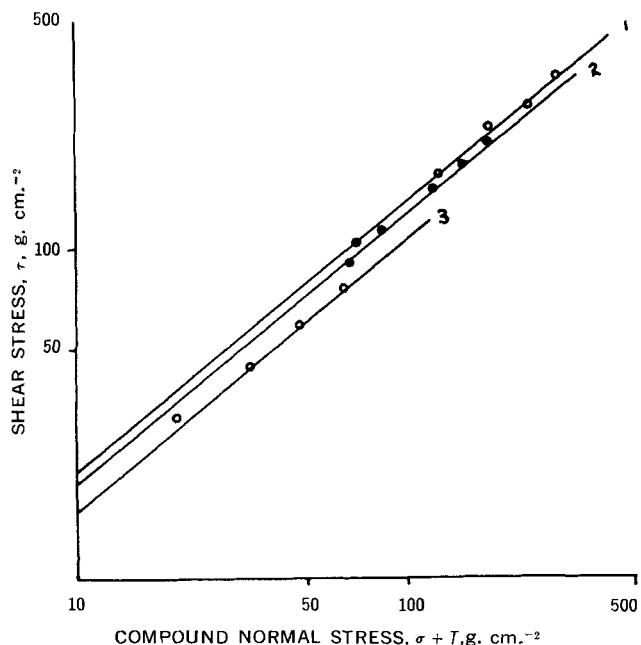


Figure 3—Logarithmic plot of shear stress versus compound normal stress for griseofulvin. Bulk density: 1., 0.567 g. cm.⁻³; 2., 0.542 g. cm.⁻³; and 3., 0.488 g. cm.⁻³.

that the yield locus can be described by the equation:

$$\left(\frac{\tau}{c}\right)^n = \frac{\sigma + T}{T} \quad (\text{Eq. 1})$$

where τ = shear stress, g./cm.²; σ = normal stress, g./cm.²; c = cohesion, g./cm.²; T = tensile strength, g./cm.²; and n = shear index.

For a great many tests on a particular material, the value of n was reported to be independent of the bulk density of the sample. The value of n was generally found to be between 1 for free-flowing powders and 2 for very cohesive powders.

Certain differences are apparent in the results found between these authors. Jenike *et al.* (1) found that the flow potential may improve with increasing compaction,

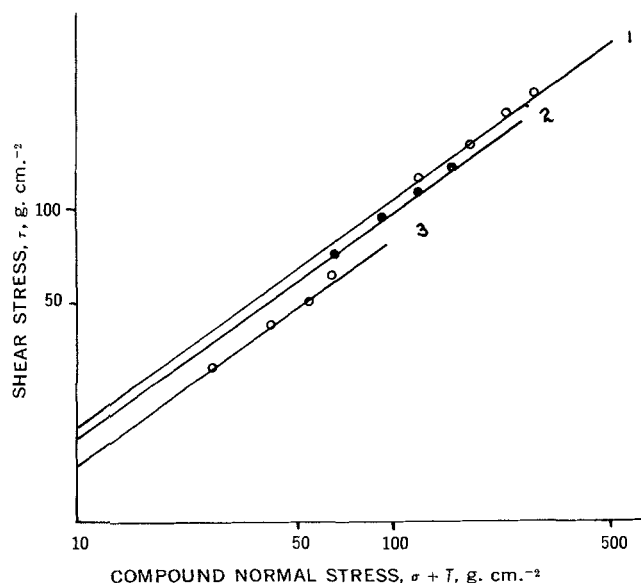


Figure 4—Logarithmic plot of shear stress versus compound normal stress for lactose.

Table I—Shear Index Value at Various Bulk Densities for Griseofulvin and Lactose

Griseofulvin		Lactose	
Bulk Density, g. cm. ⁻³	Shear Index, n	Bulk Density, g. cm. ⁻³	Shear Index, n
0.488	1.43	0.787	1.46
0.542	1.26	0.835	1.28
0.567	1.16	0.885	1.26

and this finding was substantiated by Walker (4) and the present author (5). Conversely, the results reported by Ashton *et al.* (2) suggest that the shear index is a constant, for a given powder, irrespective of the bulk density to which it is compacted.

The purpose of this communication is to point out that, in fact, the index of flow as measured by both methods does improve with increasing compaction.

Of the numerous papers on the use of the shear cell, the results of Williams and Birks (6) are particularly interesting because the normal load is reduced to the compound normal stress, that is $\sigma + T$. This results in the yield loci taking the form where all the loci have a common origin. If n were to remain constant, then all the loci would follow the same curve. It is obvious from the results of Williams and Birks (6) that the curvature is reduced with increasing compaction; thus, n must approach 1 and the flow properties must improve.

The point can be further made by considering the evidence of the measurements on a grade of lactose (average particle size 12.5 μ) and a fine grade of griseofulvin (average particle size 4 μ). Both samples were dried at 70° for 24 hr. in an air oven before being stored in vacuum desiccators until use.

The shear cell data were measured in the manner recommended by Jenike (7).

Equation 1 may be rearranged to give

$$\tau = \frac{c}{T^{1/n}} (\sigma + T)^{1/n} \quad (\text{Eq. 2})$$

By taking logarithms and plotting $\log \tau$ versus $\log (\sigma + T)$, the slope of the curves is $1/n$ and the intercept $\log c/T^{1/n}$.

The points have been plotted in Figs. 3 and 4 where it can be seen that, to a first approximation, all the curves are parallel and thus have the same value of n . However, on subjecting the values to computer analysis to find the best straight-line fit by the method of least squares, it is seen from Table I that the values of n indicate a more free-flowing condition with an increase of bulk density. This is the same result as is implicit in the treatment of Williams and Birks (6).

Thus, from the implicit data of other workers and from the experimental evidence presented here, it can be seen that both the flow factor and the shear index are in agreement in predicting an increase in the flow properties with an increase of bulk density. No explanation is offered in this brief communication, since it has merely been the purpose to point out the agreement between the two indexes. Further work is being undertaken to provide an explanation for the observed facts.

Finally, it is not suggested that a powder will be more free flowing when compacted than it is at its normal

bulk density. This is patently not true. However, its flow potential, as a relative measure, does improve as measured by the mentioned procedures.

(1) A. W. Jenike, P. J. Eysey, and R. H. Woolley, *Proc. ASTM*, **60**, 1168(1960).

(2) M. D. Ashton, O. C.-H. Cheng, R. Farley, and F. H. H. Valentin, *Rheol. Acta*, **4**, 206(1965).

(3) R. Farley and F. H. H. Valentin, *Powder Technol.*, **1**, 344 (1967).

(4) D. M. Walker, *Chem. Eng. Sci.*, **21**, 975(1966).

(5) C. F. Harwood, Ph.D. thesis, London University, London, England, 1969.

(6) J. C. Williams and A. H. Birks, *Powder Technol.*, **1**, 199(1967).

(7) A. W. Jenike, "Storage and Flow of Solids," Bulletin 123, Utah Engineering Experiment Station, University of Utah, Salt Lake City, Utah, 1964.

COLIN F. HARWOOD

IIT Research Institute
Fine Particles Research
Chicago, IL 60616

Received June 25, 1970.

Accepted for publication September 18, 1970.

GLC Analysis of the Trimethylsilyl Derivative of 2,4-Dihydroxy-3,3-dimethylbutyric Acid γ -Lactone in Pantothenyl Alcohol

Keyphrases Pantothenyl alcohol—analysis 2,4-Dihydroxy-3,3-dimethylbutyric acid γ -lactone—determination in pantothenyl alcohol GLC—analysis

Sir:

The production of *d*-pantothenyl alcohol involves the reaction between 2,4-dihydroxy-3,3-dimethylbutyric acid γ -lactone (*l*-lactone) and 2-amino-*l*-propanol (1). For manufacturing purposes, it became desirable to know the amount of residual lactone present in *d*-pantothenyl alcohol. Initial attempts to quantitate the lactone content utilized a TLC method supplied by the manufacturer¹ (2). However, the method was not completely satisfactory.

The relative volatility of the lactone (sublimes) (3) favored the investigation of GLC as a means of analysis. The initial work involved injecting pyridine solutions of known amounts of *l*-lactone and the internal standard (2,6-dimethylphenol) directly onto the GLC columns. The resulting plot of concentration *versus* peak height ratio gave a negative *y*-intercept, which suggests irreversible adsorption of the lactone. In addition, analysis of a sample of pantothenyl alcohol produced an ex-

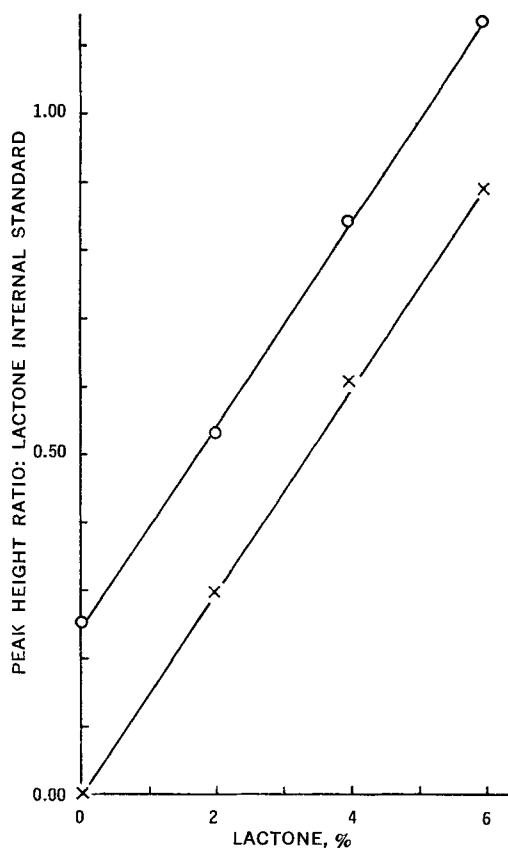


Figure 1—Key: O, lactone added to *d*-pantothenyl alcohol; and X, lactone standards.

traneous interfering peak, which we assumed to result from thermal degradation of the polyalcohol.

In an attempt to obtain a suitable chromatographic moiety, the trimethylsilyl ether derivatives of known amounts of *l*-lactone were prepared and subsequently analyzed. 2,6-Dimethylphenol was used as the internal standard. The preparation of the silyl ethers is discussed. The resulting curve of concentration *versus* peak height ratio passed through the origin and was linear, as indicated in Fig. 1.

A series of samples was run in which known amounts of *l*-lactone were added to a sample of pantothenyl alcohol, and the percent recovery was determined using the recommended procedure. In Fig. 1, the slope of the curve for *l*-lactone added to pantothenyl is essentially the same as the slope of the curve obtained in the standard calibration method. This indicates that the recovery is linear and essentially 100% relative to the normal calibration procedure.

An indication of the precision was determined by assaying three aliquots of a given sample of pantothenyl. The mean percent lactone was found to be 2.88% w/w with a standard deviation of $\pm 0.03\%$ w/w. The 2.88% is within our specifications for the sample of pantothenyl studied. The method cannot be used for resolving the *l*- and *d*-isomers of the lactone.

Basically, the method consists of weighing exactly 100 mg. of pantothenyl alcohol into a suitable vial and smearing the sample around the lower inside portion of the vial with a glass rod. A 50- μ l. aliquot of internal standard solution, prepared by dissolving 1.00 g. of

¹ Hoffmann-La Roche.